Determination of the Crystal Structure of Syndiotactic 1,2-Poly(*E*-3-methyl-1,3-pentadiene) by X-ray Diffraction and Molecular Mechanics

Beniamino Pirozzi,* Roberto Napolitano, Giovangiuseppe Giusto, and Simona Esposito

Dipartimento di Chimica "Paolo Corradini", Università di Napoli Federico II, Complesso Universitario Monte S. Angelo, via Cintia, I-80126 Napoli, Italy

Giovanni Ricci

CNR-Istituto per lo Studio delle Macromolecole (ISMAC), via Bassini 15, I-20133 Milano, Italy

Received April 24, 2007; Revised Manuscript Received October 2, 2007

ABSTRACT: The crystal structure of syndiotactic 1,2-poly(*E*-3-methyl-1,3-pentadiene) has been determined by the combination of X-ray diffraction and molecular mechanics. Energy minimizations performed by various potential functions yielded models of crystal structure with calculated X-ray powder profiles similar to the experimental profiles. The best model has been refined in order to fit all the experimental data. The space group is *Pcam*, and the parameters of the unit cell are $a = 15.4$ Å, $b = 7.45$ Å, and $c = 5.15$ Å. Similarities and differences with the crystal structures of syndiotactic 1,2-poly(1,3-butadiene), syndiotactic 3,4-poly(2-methyl-1,3-butadiene), and syndiotactic 1,2-poly(*E*-1,3-pentadiene) are discussed.

Introduction

Regular polymers with 1,2-enchainment of the three monomethyl substituted 1,3-pentadienes can have different configurations. In fact, the lateral groups can be arranged in such a way to give isotactic or syndiotactic polymers. Moreover, both the isotactic and syndiotactic polymers of 2-methyl- and of 3-methylpentadiene can have double bonds of the lateral groups in either the *cis* or *trans* configuration. In spite of the high number of possible polymers, only isotactic and syndiotactic 1,2-poly(4-methyl-1,3-pentadiene) have been synthesized up to now,[1−5] and only the crystal structure of the latter has been reported.[6−7]

A previous paper[8] reports the polymerization of a mixture of *E* and *Z* isomers of 3-methyl-1,3-pentadiene and the characterization of the resulting polymer. The synthesis was performed using a catalyst system based on $FeCl_2(bipy)_2$ and methylaluminoxane. Characterization by nuclear magnetic resonance (solution ^1H and ^{13}C NMR and solid-state ^{13}C NMR), infrared spectroscopy, X-ray diffraction, differential scanning calorimetry (DSC) and gel permeation chromatography has assigned the obtained polymer a 1,2-syndiotactic structure with the methyl groups of the lateral groups in *cis* configuration, i.e., the obtained polymer is syndiotactic 1,2-poly(*E*-3-methyl-1,3-pentadiene) [sEP3MPD12].

This paper reports the crystal structure of sEP3MPD12 as determined by the combination of a detailed X-ray characterization of powder and fiber samples and of molecular mechanics. A critical comparative analysis is also conducted of this crystal structure with those of syndiotactic 1,2-poly(1,3-butadiene)[9] [sPBD12], syndiotactic 3,4-poly(3-methyl-1,3-butadiene)[10] [sPMBD34], and syndiotactic 1,2-poly(*E*-1,3-pentadiene)[11] [sEPPD12]. The comparison is justified because sPMBD34, sEPPD12, and sEP3MPD12 can be considered to be derived from sPBD12 by the substitution of one or two hydrogen atoms of the side groups with methyl groups.

* Corresponding author. Fax: +39 081674300. E-mail: Beniamino.Pirozzi@unina.it.

Experimental Part

The polymer samples were synthesized as described in a previous paper.[8] DSC measurements were performed by a Mettler calorimeter at a scanning rate of 10 °C/min. The density of the polymer sample was determined by flotation. The as prepared sample was subjected to various thermal and mechanical treatments: (i) melting under pressure followed by slow cooling under pressure; (ii) cooling without pressure; (iii) quenching in a mixture of ice and water. X-ray measurements were carried out using Ni-filtered Cu Kα radiation ($\lambda = 1.5418$ Å). Powder spectra were collected by a Philips PW3710 automated diffractometer operating in the conventional $\theta/2\theta$ Bragg−Brentano geometry. An Anton-Paar TTK 450 low-temperature camera was used for the X-ray measurements at various temperatures. A Pt_{100} thermocouple inserted into the sample holder was used for high-precision measurements and for the control of the working temperature. Fibers of the polymer sample were obtained by the following procedure: samples of the as-prepared polymer were extruded by a syringe, stretched by 200% and annealed at various temperatures and for different times. Annealing temperatures greater than 140 °C were not reached because the fiber samples broke in few minutes. Fiber spectra were collected by a cylindrical camera ($r = 57.3$ cm); for these spectra the Cu Kα radiation was monochromatized with a graphite crystal. The Fuji film MS 2025 imaging plate and the Fuji Bioimaging analyzer System, mod. BAS-1800, were used for digitizing the diffraction patterns.

All the calculations of the internal energy and of the diffraction spectra were performed using the Cerius^2 program (Accelrys). The crystals were generated by the *Crystal Builder* module and the *Analytical* module was used to calculate the X-ray diffraction spectra. The isotropic thermal factor $B = 12$ Å^2 was adopted for all the spectra. The crystal sizes $a = 150$ Å, $b = 150$ Å, $c = 60$ Å and $a = 300$ Å, $b = 300$ Å, $c = 80$ Å were used in the calculated powder and fiber spectra, respectively. The energy was minimized using the *Open Force Field* module by the *smart minimizer* method with *standard convergence*. The following force fields were used: Universal1.02,[12] UFF_Valbond,[13] Dreiding,[14] and Compass.[15] The electrostatic term was calculated for the Dreiding and Compass force fields. Gasteiger[16] estimates for charges were taken into account for the Dreiding field, while the Compass force field has its own method of calculating the electrostatic charges.

10.1021/ma070951y CCC: $37.00
Published on Web 11/14/2007

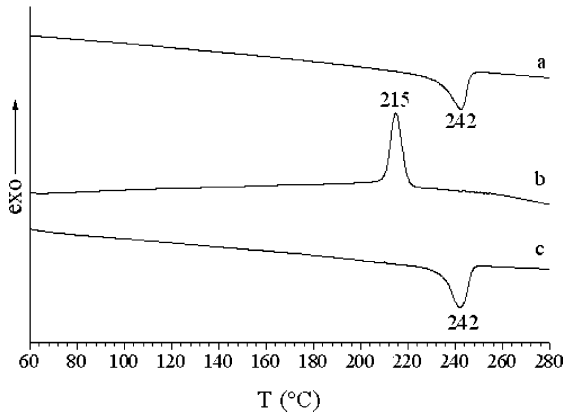

Figure 1. DSC traces of sEP3MPD12 obtained by heating the as-prepared sample up to ~30 °C above the melting temperature (a), cooling the melt down to room temperature (b), and heating the bulk crystallized sample up to ~30 °C above the melting temperature (c).

Sample Characterization

Figure 1 shows the DSC traces obtained by heating the as-prepared sample up to ~30 °C above the melting temperature (a), cooling the melt down to room temperature (b) and heating the bulk crystallized sample up to ~30 °C above the melting temperature (c). Both the as-prepared and the bulk crystallized samples exhibit only one endothermic peak, practically at the same temperature. An exothermic peak is observed at a lower temperature during the cooling of the melt sample. Figure 2 shows the X-ray powder spectra of the as-prepared sample (a), of the melted and pressurized slow cooled sample (b), and of the melted and quenched sample (c). The profile of the melt sample, assumed as the profile of the amorphous phase, is also reported in each spectrum. The crystallinity calculated from the ratio between the crystalline and total area is also indicated for each sample. The sample crystallized from the bulk without pressure is not reported because it exhibits the same profile as the spectrum of Figure 2b. This profile appears significantly different with respect to the profile of the as-prepared sample. In fact, it exhibits more resolved reflections and shows larger crystal sizes. At variance, the melted and quenched sample exhibits a profile similar to that of the as-prepared sample despite the lower crystallinity value. The results of the DSC and X-ray analyses indicate that the polymer crystallizes rapidly, independently of the mechanical and thermal treatments.

In order to determine the crystal structure of sEP3MPD12 and to observe structural changes as a function of temperature, the X-ray powder spectra of the melted and slowly cooled sample were also collected at various temperatures up to the melting point. Detailed collections were performed with a step size of 0.04° and a step time of 44 s in order to obtain accurate values of the axes of the unit cell. Figure 3 shows the X-ray powder profiles at the various temperatures. Neither the X-ray profiles or the DSC traces show evidence of polymorphism in samples of sEP3MPBD12 crystallized from the bulk.

Figure 4 shows the spectrum of a fiber sample annealed at 140 °C for 1 h, obtained by the cylindrical camera. The fiber sample appears well oriented and its spectrum exhibits several equatorial reflections but a low number of layer reflections. However, the analysis of the fiber spectrum has allowed for the determination of the value of the *c* axis, which is 5.15 ± 0.05 Å. Figure 5 shows the equatorial profile of the fiber spectrum. The resolution and the positions of the maxima of the two most intense reflections are more similar to those of the as-prepared sample rather than to those of the samples crystallized from the bulk.

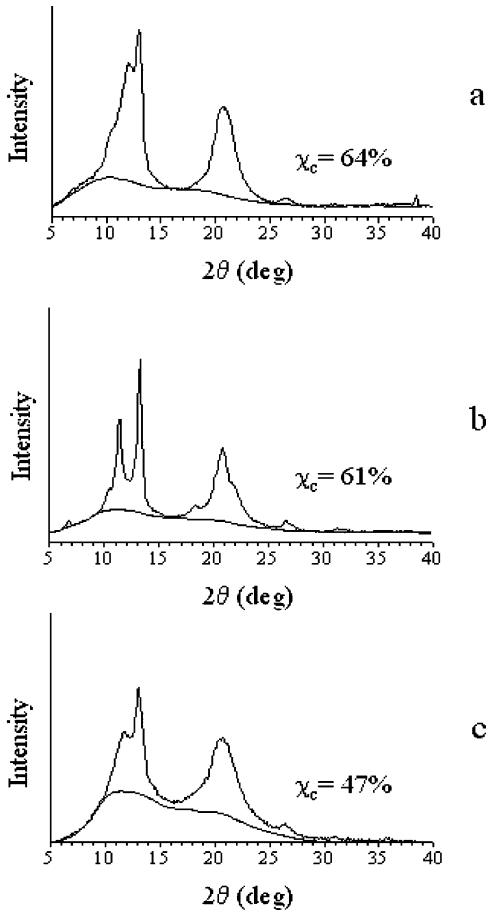

Figure 2. X-ray powder spectra of samples of sEP3MPD12: (a) as-prepared sample; (b) sample melted and slowly cooled under pressure; (c) sample melted and quenched in a mixture of ice and water. The curve of the amorphous phase and the value of the crystallinity, χ_c, are also reported for each sample.

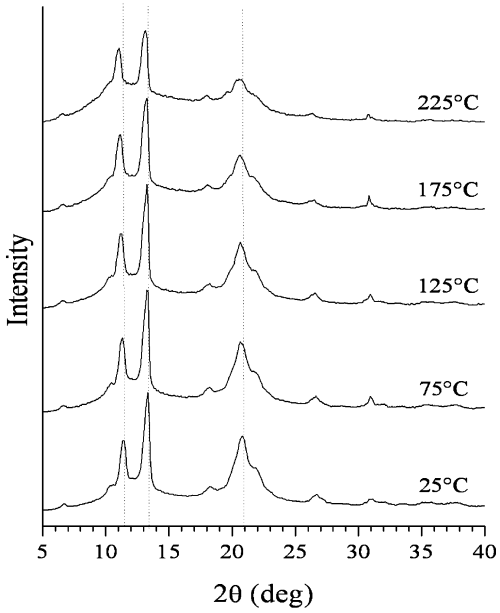

Figure 3. X-ray powder spectra of sEP3MPD12 collected at the indicated temperatures.

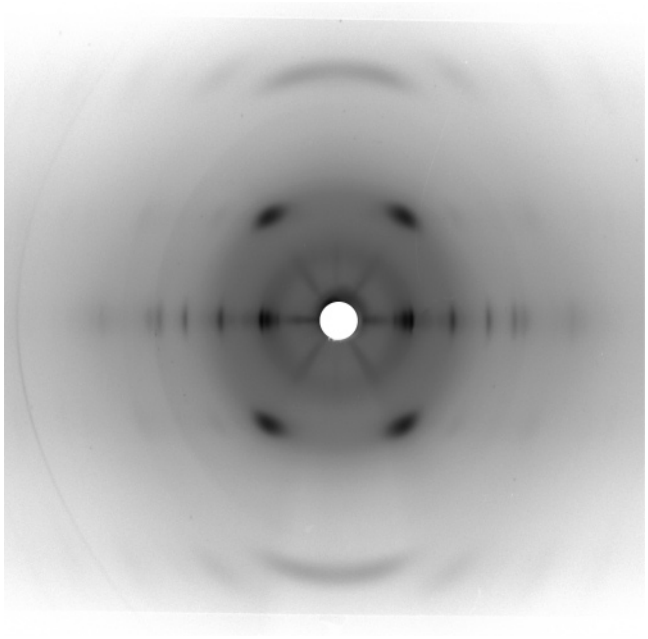

Figure 4. X−ray fiber spectrum of sEP3MPD12 collected by the cylindrical camera.

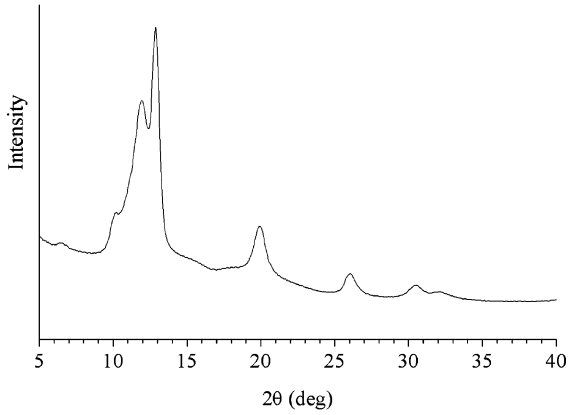

Figure 5. Equatorial profile of the fiber spectrum of sEP3MPD12.

Crystal Structure

The determination of the crystal structure was first undertaken by molecular mechanics calculations in order to obtain structural models which compare calculated X-ray spectra with the experimental spectrum of the melted and slowly cooled sample. The most promising model has been successively refined in order to obtain the best agreement with all the experimental data.

Previously reported molecular mechanics calculations performed on an isolated chain of sEP3MPD12 indicated that the minimum energy chain conformation is highly extended.[17] Moreover, the experimental value of the *c* axis (5.15 Å) determined here is compatible with the **t***cm* symmetry of the chain. This chain symmetry is characterized by a glide plane containing the chain axis and by mirror planes perpendicular to it which contain the atoms of the lateral groups. The independent parameters of the backbone of a chain having **t***cm* symmetry are one bond length, two bond angles, and one torsion angle.[18] Figure 6 shows a portion of the chain of sEP3MPD12 made up of two monomeric units, with the independent bond and torsion angles and the numbering of the carbon atoms of the asymmetric unit indicated. The present calculations take all the orthorhombic space groups in which the symmetry elements

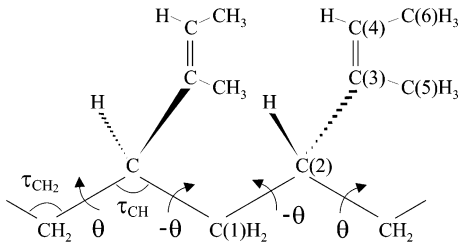

Figure 6. Portion of the chain of sEP3MPD12 made up of two monomeric units, with the independent bond and torsion angles indicated and with the carbon atoms of the asymmetric unit numbered.

Table 1. Values of the Optimized Energy (kcal/mol of Unit Cell) Obtained by the Minimization of the Internal Energy of the Models of Crystal Structure of sEP3MPD12 in the Indicated Space Groups, Performed by Various Force Fields

force field	$Pmc2_1$	$Pnc2$	$Pccm$	$Pcam$
Universal 1.02	18.06	11.82	19.78	4.23
UFF_Valbond	7.88	2.98	8.14	−8.22
Dreiding	71.55	67.44	70.11	60.19
Compass	−51.65	−55.90	−45.16	−55.64

Table 2. Values of the Bond and Torsion Angles of the Backbone and of the *a* and *b* Axes of the Unit Cell Obtained by the Minimization of the Internal Energy of the Models of Crystal Structure of sEP3MPD12 in the *Pcam* Space Group, Performed by Various Force Fields

force field	τ_{CH}/deg	τ_{CH_2}/deg	θ/deg	*a*/Å	*b*/Å
Universal 1.02	112.0	112.1°	−176.4	13.76	7.90
UFF_Valbond	113.2	113.5	−173.9°	13.74	7.93
Dreiding	111.4	112.4	−168.6°	15.05	7.41
Compass	113.1	113.2	−176.0°	14.05	7.31

of the chain are also crystallographic symmetry elements. Moreover, according to the experimental density, the unit cell must contain two chains. The space groups which satisfy these requirements are $Pmc2_1$, $Pnc2$, $Pccm$, and $Pcam$.[19] The crystal structure of sPMBD34[10] has been used as the starting point of the minimizations in the *Pcam* space group, modifying its polymer chain by the substitution of suitable hydrogen atoms with methyl groups. The starting points for the other space groups have been obtained modifying the crystal structure of the *Pcam* space group by suitable changes of the positions of the chains in the unit cell. The internal energy of the crystal has been minimized as a function both of the fractional coordinates of the atoms and of the *a* and *b* axes of the unit cell, with the *c* axis fixed at the experimental value. Table 1 shows the values of the optimized energy of the models of crystal structure of sEP3MPD12 in the quoted space groups, obtained by the various force fields. The results of Table 1 clearly indicate that the best mode of packing is realized in the *Pcam* space group. Moreover, the calculated powder spectra for this space group are in better accordance with the experimental powder spectrum.[20] The *Pcam* space group was already found in the crystal structures of sPBD12,[9] sPMBD34,[10] and sEPPD12,[11] polymers having constitutional, configurational and conformational similarities with sEP3MPD12.[21] The optimized values of the bond and torsion angles of the backbone and of the parameters *a* and *b* of the unit cell obtained by the various force fields for the *Pcam* space group are shown in Table 2. There is good agreement between the optimized values obtained by the various force fields. In fact, the values of the conformational parameters are very similar and the highest deviations from the mean values for the axes of the unit cell are 0.90 Å and 0.33 Å for *a* and *b*, respectively.

Figure 7 shows the calculated powder spectra of sEP3MPD12 corresponding to the models of minimum energy crystal

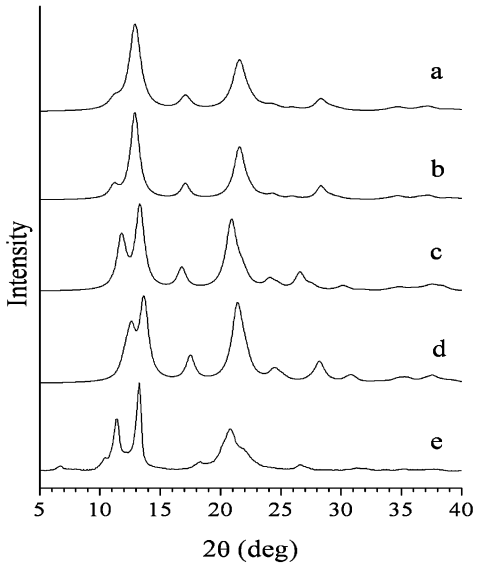

Figure 7. Calculated powder spectra of sEP3MPD12 using the models of minimum energy crystal structure in the *Pcam* space group obtained by the various sets of potential functions [(a) Universal 1.02; (b) UFF_Valbond; (c) Dreiding; (d) Compass], in comparison with the spectrum of the crystal phase (e) obtained by subtraction of the contribution of the amorphous phase from the experimental spectrum of the melted and slowly cooled sample.

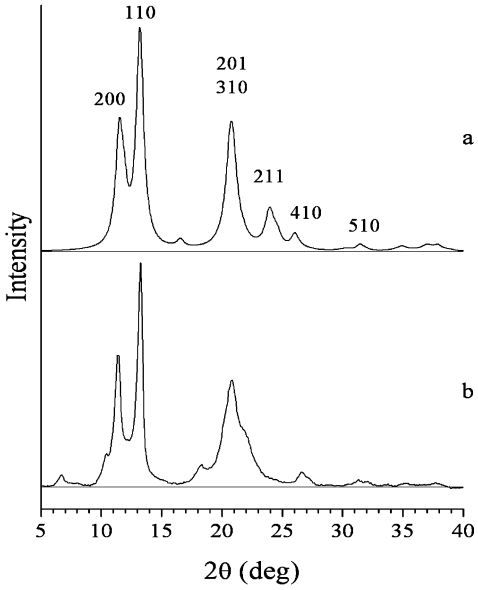

Figure 8. (a) Calculated powder spectrum of the refined model of the crystal structure of sEP3MPD12, with the indices of the most intense reflections indicated; (b) spectrum of the crystal phase.

structure in the *Pcam* space group obtained by the various potential functions, in comparison with the spectrum of the crystal phase obtained by subtraction of the contribution of the amorphous phase from the experimental spectrum of the melted and slowly cooled sample. All the calculated spectra are similar to the experimental spectrum of the crystal phase as whole, even if spectrum c of Figure 7 is in better agreement with both the positions and the intensities of the reflections. Therefore, the model corresponding to spectrum c has been chosen as the starting point for the refinement of the crystal structure of sEP3MPD12. The refinement has been carried out giving trial values to *a* and *b* in order to obtain the best accordance between the 2θ values of the calculated and observed reflections. For each pair of *a* and *b* the energy of the model of crystal structure has been optimized, by using the Dreiding force field, under

Figure 9. Calculated fiber spectrum of the refined model of the crystal structure of sEP3MPD12.

Table 3. Indices and Corresponding Values of 2θ (deg) and of the Intensity for the Calculated and Observed Reflections in the Powder Spectra. The Observed Values of 2θ of the Most Intense Reflections of the Fiber Spectrum Are Also Reported

hkl	$2\theta_c$	$2\theta_o$	I_c	I_o	$2\theta_o$(fiber)
		6.8	0	24	6.6
		10.5	0	23	10.1
200	11.49	11.4	306	307	11.9
010	11.88				
110	13.20	13.2	437	416	12.9
210	16.57	*a*	13	*b*	15.7
		18.4	0	23	
201	20.75	20.8	357	427	20.8
310	21.02				19.9
211	23.97	*c*	139	218	*d*
410	26.05	26.6	44	42	26.1
510	31.43	31.3	26	32	30.5

[a] Comprised between 15 and 17°, but not well-defined. [b] Very weak, evaluated as 0 in the calculation of R. [c] Comprised between 22.5 and 24.5°, but not well-defined. [d] Comprised between 23 and 24°, but not well-defined.

the constraint of the *Pcam* space group, and the powder spectrum corresponding to the minimum energy has been calculated and compared with the experimental spectrum. The discrepancy factor has been calculated as $R = (\Sigma|I_o - I_c|/\Sigma I_o) \times 100$, where I_o and I_c are the intensities of the observed and calculated reflections, respectively. I_o and I_c have been obtained evaluating (by weight determinations) the areas of the reflections, corrected by a scale factor estimated as the ratio between the total areas of the experimental and calculated powder profiles.

Figure 8 shows the calculated powder spectrum of the refined model in comparison with the experimental spectrum, with the indices of the most intense reflections indicated. Figure 9 shows the calculated fiber spectrum which also is in quite good agreement with the experimental fiber spectrum. Table 3 shows the indices and the corresponding values of 2θ and of the intensity for the calculated and observed reflections in the powder spectra. The observed values of 2θ of the most intense reflections of the fiber spectrum are also reported in Table 3. The agreement between the calculated and observed reflections of the powder spectra is good both for the positions and for the intensities of most reflections. Discrepancies appears for the

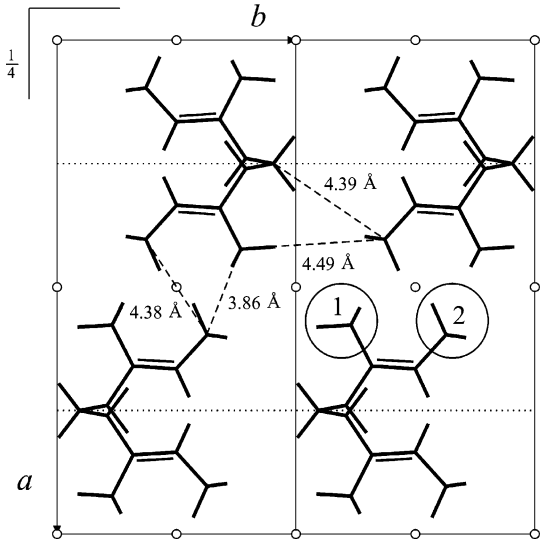

Figure 10. Projection along the *c* direction of the content of two unit cells of the refined crystal structure of sEP3MPD12. The shortest intermolecular distances between carbon atoms and the main symmetry elements of the *Pcam* space group are also indicated. Circles enclose the methyl groups of an asymmetric unit.

Table 4. Values of the Fractional Coordinates of Carbon Atoms of the Asymmetric Unit in the Crystal Structure of sEP3MPD12

	x	*y*	*z*
C(1)	0.250	0.906	0.500
C(2)	0.260	0.791	0.250
C(3)	0.340	0.681	0.250
C(4)	0.334	0.501	0.250
C(5)	0.423	0.770	0.250
C(6)	0.403	0.372	0.250

very low intense reflections at $2\theta = 6.8$, 10.5, and 18.4°, which are observed but not calculated.[22] In any case these reflections have been taken into account in the evaluation of R. The resulting value of R is 17%, and the final values of the parameters of the unit cell are $a = (15.4 \pm 0.2)$ Å, $b = (7.45 \pm 0.10)$ Å, and $c = (5.15 \pm 0.05)$ Å. The calculated density is 0.92 g·cm^{-3}, in good agreement with the experimental value of the density of the semicrystalline polymer, 0.91 g·cm^{-3}. Table 4 shows the fractional coordinates of the carbon atoms of the asymmetric unit. Figure 10 shows the projection along the *c* axis of the content of two unit cells of the refined crystal structure of sEP3MPD12, with the shortest intermolecular distances between carbon atoms indicated.

The values of the *a* and *b* axes of the unit cell have been determined at various temperatures by analyzing the X-ray powder profiles shown in Figure 3. The 200 and 110 reflections were chosen because they are the only equatorial intense reflections. At each temperature the value of the *a* axis has been directly determined from the 2θ value of the 200 reflection, while the value of the *b* axis has been obtained from the 2θ value of the 110 reflection using the value of the *a* axis at the same temperature. The values of the *a* and *b* axes as a function of temperature are shown in Figure 11. The trends are linear, so constant values of the thermal expansion coefficients of the *a* and *b* axes have been obtained, and they are $\lambda_a = 1.6 \times 10^{-4}$ K^{-1} and $\lambda_b = 3.1 \times 10^{-5}$ K^{-1}, respectively. The value of the thermal expansion coefficient of the *c* axis is not easily obtainable because the X-ray powder profile does not have isolated nonequatorial reflections. On the other hand, the value of the *c* axis depends only on chain conformation and is generally invariant with temperature. The invariance of *c* with temperature was verified for other polymers, as reported in

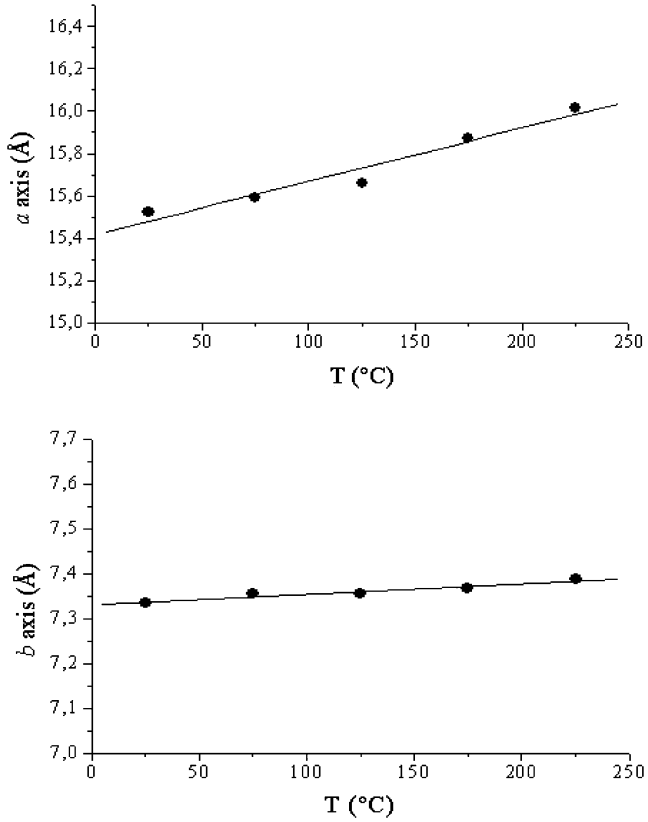

Figure 11. Values of the *a* and *b* axes of the unit cell of sEP3MPD12 as a function of temperature.

previous papers.[23−26] The values of λ_a and λ_b allow to calculate the lengths of *a* and *b* at 0 K. They are $a = 14.7$ Å and $b = 7.38$ Å in quite good agreement with those calculated by the Dreiding and Compass force fields.

Discussion

The powder spectra of the as-prepared sample (Figure 2a) and of the melted and quenched sample (Figure 2c) are very similar, but they are rather different from the spectrum of the non-quenched samples crystallized from the bulk at different rates (Figure 2b). In particular, the two most intense reflections, having indices 200 and 110, are more resolved in the spectrum of Figure 2b. The resolution of these reflections is due to a decrease of the 2θ value of the maximum of the 200 reflection and to an increase of the 2θ value of the maximum of the 110 reflection. The resolution of reflections in the X-ray spectra of polymer samples generally increases with the decrease of the crystallization rate and can be ascribed to the larger crystal size of the slowly crystallized samples. In this case, the width of the resolution is higher than expected. Therefore, we think that for sEP3MPD12 during slow crystallization, together with the increase of crystal size, a more efficient packing is realized along the *b* direction which leads to a lowering of the *b* value and consequently an increase of the *a* value, i.e., a lowering of the 2θ value of the 200 reflection. However, the packing of the chains along the *b* direction is still rather large as shown by the high values of the shortest distances between carbon atoms along this direction (see Figure 10) and confirmed by the value of λ_b, which is lower with respect to both the value of λ_a and to the thermal expansion coefficients of other polymers.[23−26] Also the two most intense reflections of the equatorial profile of the fiber spectrum (Figure 5) are less resolved than the corresponding reflections of the powder spectra of the samples crystallized from the bulk. This could be due to the very high cooling rate

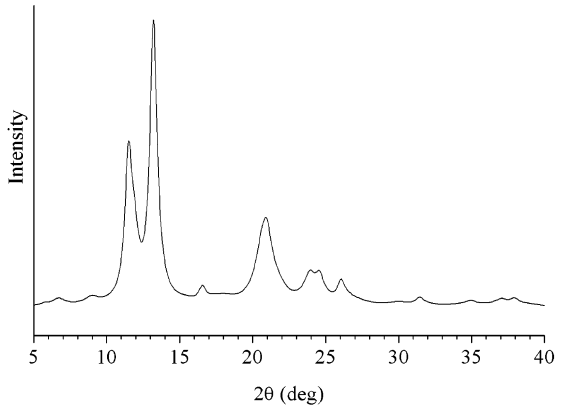

Figure 12. Calculated powder spectrum of the model of crystal structure sEP3MPD12 including 1 meso diad every 20 monomeric units as defect.

Table 5. Values of the Axes of the Unit Cells of the Indicated Polymers

	a/Å	*b*/Å	*c*/Å
sPBD12	10.98	6.60	5.14
sPMBD34	13.2	6.6	5.27
sEPPD12	14.69	6.59	5.11
sEP3MPD12	15.4	7.45	5.15

during extrusion from the syringe, which was more similar to that of the quenched sample than to those of the samples crystallized from the bulk. Therefore, the ideal crystal structure, rather different from the structure of rapid crystallized samples, exhibits 2θ values of the reflections in less satisfactory agreement with those of the experimental fiber spectrum.

The not efficient packing of this crystal structure, especially along the *b* direction, could derive by the inclusion in the crystal phase of configurational defects which cause conformational changes in the chains in such a way that they become locally less extended. As reported in a previous paper,[8] the most probable configurational defects in this polymer sample are the meso diads. Therefore, models of crystal structure of sEP3MPD12 with various amounts of meso diads have been taken into account. They have built up and minimized by the Dreiding force field following the procedure described in a previous paper.[27] For each model the powder spectrum has been calculated and compared with the experimental powder spectrum. The calculated powder spectrum for chains containing one meso diad every 20 monomeric units is reported in Figure 12. The R factor calculated for the powder spectrum of this model of crystal structure is slightly higher with respect to that calculated for the ideal crystal structure. However, this powder spectrum exhibits very low intense reflections at $2\theta \sim 7°$, $\sim 9°$, and $\sim 18°$, near the 2θ values of the three observed reflections not calculated for the ideal crystal structure (see Table 3). Hence, we think that these three reflections are due to a spurious crystal phase containing meso diads in some amount.

The crystal structures of sEP3MPD12, sPBD12, sPMBD34, and sEPPD12 can be compared. All these polymers crystallize with an orthorhombic unit cell in the *Pcam* space group with chains having **t***cm* symmetry. As already underlined, these polymers are analogous in their constitution. In fact, the two methyl groups of an asymmetric unit of sEP3MPD12, circled and indicated by 1 and 2 in Figure 10, correspond to hydrogen atoms in sPBD12, while only the methyl group 2 in sPMBD34 and only the methyl group 1 in sEPPD12 correspond to hydrogen atoms. The value of the axes of the unit cell of these polymers are reported in Table 5. The values of the *c* axes are very similar because in the highly extended chains of these polymers, the adjacent lateral groups are so far apart that the presence of methyl groups instead of hydrogen atoms does not imply repulsive interactions. On the contrary, the value of the *b* axis of sEP3MPD12 is significantly higher with respect to that of the other three polymers. This can be explained considering that repulsive intermolecular interactions along the *b* direction only arise if both the hydrogen atoms of the lateral group of sPBD12 are substituted by methyl groups. The differences between the values of the *a* axes of the four polymers can be also explained by the different number of methyl groups in the lateral group. In fact, the value of *a* increases from sPBD12 (no methyl group) to sPMBD34 and sEPPD12 (one methyl group) and further to sEP3MPD12 (two methyl groups). The substitution of each hydrogen atom by a methyl group causes in each case repulsive intermolecular interactions along the *a* direction. The higher value of *a* of sEPPD12 with respect to that of sPMBD34 can be attributed to the different position of the only methyl group in the side chain, which in the case of sPMBD34 (corresponding to the methyl group 1 in Figure 10) better lodges with the two chains of the adjacent *b* layer.

Conclusions

The crystal structure of sEP3MPD12 was determined by the combination of X-ray diffraction and molecular mechanics. It is characterized by highly extended chains that maintain their symmetry elements in the crystal. Structural analogies with sPBD12, sPMBD34 and sEPPD12 have been found both in the chain conformation and in the mode of packing of the chains, which are in layers along the *b* direction. On the other hand, the values of the *a* and *b* axis of the unit cell of sEP3MPD12 are larger with respect to those of the other three polymers. This is due to the presence of two methyl groups in the lateral group of the polymer chain instead of one or two hydrogen atoms, which requires larger distances between chains within the same layer and between layers. X-ray measurements performed over a large range of temperatures shows that the only changes in the crystal structure of sEP3MPD12 are the expansions of the *a* and *b* axes of the unit cell with temperature. The rather low value of the thermal expansion coefficient of the *b* axis has been related to the high values of the shortest distances between the atoms of adjacent chains inside the same layer in the crystal structure of sEP3MPD12.

Acknowledgment. This work was supported by the Ministero dell'Istruzione, dell'Università e della Ricerca (Italy), PRIN 2004.

Supporting Information Available: Figures showing the calculated powder spectra for the *Pmc*2_1, *Pnc*2, and *Pccm* space groups. This material is available free of charge via the Internet at http://pubs.acs.org.

References and Notes

(1) Porri, L.; Gallazzi, M. C. *Eur. Polym. J.* **1966**, *2*, 189.
(2) Zambelli, A.; Ammendola, P.; Proto, A. *Macromolecules* **1989**, *22*, 2126.
(3) Oliva, L.; Longo, P.; Grassi, A.; Ammendola, P.; Pellecchia, C. *Makromol. Chem., Rapid Commun.* **1990**, *11*, 519.
(4) Ricci, G.; Italia, S.; Giarrusso, A.; Porri, L. *J. Organomet. Chem.* **1993**, *451*, 67.
(5) Ricci, G.; Porri, L.; Giarrusso, A. *Macromol. Symp.* **1995**, *89*, 383.
(6) Meille, S. V.; Capelli, S.; Ricci, G. *Macromol. Rapid Commun.* **1995**, *16*, 891.
(7) Immirzi, A.; Tedesco, C.; Meille, S. V.; Famulari, A.; van Smaalen, S. *Macromolecules* **2003**, *36*, 3666.

(8) Ricci, G.; Bertini, F.; Boccia, A. C.; Zetta, L.; Alberti, E.; Pirozzi, B.; Giarrusso, A.; Porri, L. *Macromolecules*, **2007**, *40*, 7238.
(9) Natta, G.; Corradini, P. *J. Polym. Sci.* **1956**, *20*, 251.
(10) Pirozzi, B.; Napolitano, R.; Petraccone, V.; Esposito, S. *Macromol. Chem. Phys.* **2004**, *205*, 1343.
(11) Ricci, G.; Motta, T.; Boglia, A.; Alberti, E.; Zetta, L.; Bertini, F.; Arosio, P.; Famulari, A.; Meille, S. V. *Macromolecules* **2005**, *38*, 8345.
(12) Rappé, A. K.; Casewit, C. J.; Colwell, K. S.; Goddard, W. A., III; Skiff, W. M. *J. Am. Chem. Soc.* **1992**, *114*, 10024.
(13) Root, D. M.; Landis, C. R.; Cleveland, T. *J. Am. Chem. Soc.* **1993**, *115*, 4201.
(14) Mayo, S. L.; Olafson, B. D.; Goddard, W. A, III. *J. Phys. Chem.* **1990**, *94*, 8897.
(15) Sun, H. *J. Phys. Chem. B* **1998**, *102*, 7338.
(16) Gasteiger, J.; Marsili, M. *Tetrahedron* **1980**, *36*, 3219.
(17) Pirozzi, B.; Napolitano, R.; Esposito, S. *Macromol. Theory Simul.* **2004**, *13*, 679.
(18) Corradini, P.; Napolitano, R.; Pirozzi, B. *Eur. Polym. J.* **1990**, *26*, 157.
(19) Hahn, T., Ed. International Tables for Crystallography; Kluwer Academic Publishers: Dordrecht, The Netherlands, 2002.
(20) The calculated spectra for the $Pmc2_1$, $Pnc2$, and $Pccm$ space groups are available as Supporting Information. The calculated spectra for the *Pcam* space group are shown in Figure 7.
(21) Really, the space group proposed in refs 10 and 11 is *Pbcm*, which corresponds to *Pcam* if an exchange between the *a* and *b* axes is effected.
(22) Attempts to remove these discrepancies were made considering models of crystal structure in which the chains have higher freedom degrees. To this end, the monoclinic $P2_1/c$ space group, in which the chain symmetry is reduced to **t***c* and the chains can incline and shift along *c*, has been taken into account. However, in the minimum energy points, calculated for the $P2_1/c$ space group by the various force fields, the chains assume the **t***cm* symmetry and pack practically as in the *Pcam* space group. Obviously, the discrepancies between the calculated and the experimental powder spectra remain.
(23) Aronne, A.; Napolitano, R.; Pirozzi, B. *Eur. Polym. J.* **1986**, *22*, 703.
(24) Napolitano, R.; Pirozzi, B.; Varriale, V. *J. Polym. Sci., Polym. Phys.* **1990**, *28*, 139.
(25) Napolitano, R.; Pirozzi, B.; Iannelli, P. *Macromol. Theory Simul.* **2001**, *10*, 827.
(26) Napolitano, R.; Pirozzi, B.; Esposito, S. *Macromol. Symp.* **2006**, *234*, 111.
(27) Napolitano, R.; Pirozzi, B.; Esposito, S. *Macromol. Chem. Phys.* **2006**, *207*, 503.

MA070951Y